CHAPTER 6

Effects of Substrate and Polymer encapsulation on CO_2 Electroreduction by Immobilized Indium(III) protoporphyrin

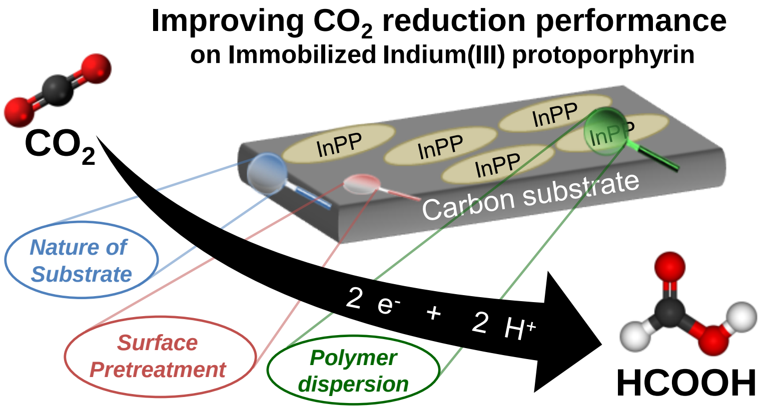

This chapter is based on the article:
Yuvraj Y. Birdja, Rafaël E. Vos, Tim A. Wezendonk, Lin Jiang, Freek Kapteijn and Marc T. M. Koper, ACS Catal., under revision

Abstract

Heterogenization of molecular catalysts for CO_2 electroreduction has attracted significant research activity, due to the combined advantages of homogeneous and heterogeneous catalysts. In this work, we demonstrate the strong influence of the nature of the substrate on the selectivity and reactivity of electrocatalytic CO_2 reduction, as well as on the stability of the studied immobilized indium(III) protoporphyrin IX, for electrosynthesis of formic acid. Additionally, we investigate strategies to improve the CO_2 reduction by tuning chemical functionality of the substrate surface by means of electrochemical and plasma treatment, and by catalyst encapsulation in polymer membranes. We point out several underlying factors that affect the performance of electrocatalytic CO_2 reduction. The insights gained here, allow one to optimize heterogenized molecular systems for enhanced CO_2 electroreduction without modification of the catalyst itself.

6.1 Introduction

The electrocatalytic reduction of carbon dioxide (CO_2RR) is a potentially efficacious strategy to tackle the global energy concerns, particularly, to close the carbon cycle, and store renewable electrical energy in chemicals or fuels.[1] The latter is highly desired due to the intermittent character of renewable energy production. The last decades have experienced the discovery and development of various electrocatalysts, which all lead to a diversity of products with different selectivity and activity.[2–4] Besides heterogeneous CO_2 electrocatalysis using metal, metal alloy, or metal-derived, nanostructured electrocatalysts, molecular catalysis of CO_2 has shown interesting properties, and have undergone a striking development over the years..[5–8] Molecular catalysts are generally considered to yield high selectivity and activity, and can be designed in such a way to mimick enzymes used in nature to efficiently catalyze specific electrochemical reactions such as hydrogen evolution, water oxidation, carbon dioxide reduction, and oxygen reduction.[6,9] Although their stability and solubility in aqueous electrolytes and their poor robustness are often drawbacks, molecular catalysts are widely used to decipher mechanistic insight due to their well-known molecular structure and their efficiency. Hence, many studies have been performed on intrinsic catalyst properties such as the influence of the metal center[10–12] and ligands.[13–17] The focus herein will be on metalloporphyrins, a subgroup of molecular catalysts extensively used for CO_2RR research.[18,19] In previous work, we reported that cobalt(II) and indium(III) protoporphyrin IX (InPP) immobilized on pyrolytic graphite exhibit high selectivity toward carbon monoxide and formic acid, respectively.[12,20]

The usually poor solubility of molecular catalysts in aqueous media, and need for large amounts of catalyst related to homogeneous molecular catalysts, can be overcome by heterogenization. The molecular catalyst is immobilized on a conductive electrode, which we will refer to as ”the substrate” in the remainder of this article. An additional advantage of immobilization of the catalyst is the more facile product separation, if utilized in a large-scale industrial process. Carbon materials are often employed as substrate owing to their relatively low cost, robustness and inert nature toward many (electro)chemical reactions. Examples are pyrolytic graphite, glassy carbon and more recently boron doped diamond, carbon nanotubes, and graphene.[21–23] Carbon materials exhibit a rich surface chemistry, and their surface functionalization has been proved to play an important role in their electrochemistry.[24] Studies by Morozan et al. and Rigsby et al. demonstrate the important influence of the carbon support of porphyrins on the selectivity of the oxygen reduction reaction.[22,25] Magdesieva et al. reported on activated carbon supports with different pore sizes for CO_2RR on various porphyrin and phthalocyanine complexes, leading to different selectivity.[26] However, little systematic or comparative work has been performed hitherto, to elucidate the intrinsic influence of the substrate or surface functionalization. The choice of a specific substrate is often solely based on empirical considerations, which not necessarily is the optimal system.

Modification of electrodes started in the early '80s with several methods such as chemisorption or covalent attachment of species on the electrode surface, encapsulation of species in polymer films, or electropolymerization of monomers directly on the electrode..[27,28] More recently, Yaghi and coworkers developed a covalent organic framework of porphyrin building blocks, which showed promising results for CO_2RR.[29] An overview of various catalyst-modified electrodes for CO_2RR has been given by Sun et al.[30] From heterogeneous electrocatalysis of CO_2RR, it is known that the electrode morphology and (sub)surface structure significantly influence the activity and selectivity.[31–33] Moreover, the use of polymers has been shown to enhance CO_2RR efficiency on cobalt phthalocyanines.[34–36] In the field of heterogenized molecular catalysis of CO_2RR, the effects of such substrate modifications are still unexplored. The importance of chemical functionality on the adsorption and reactivity, as extensively discussed by McCreery,[24] is the inspiration of the idea that substrate modification may impact the reactivity, selectivity, and stability of CO_2RR. In a recent review, the importance of so-called secondary phenomena in molecular electrocatalysis have been highlighted.[37] It would be very attractive to be able to tailor the surface chemistry in such way, to enhance CO_2RR performance.

In this study we focus on extrinsic properties of the molecular catalyst, particularly related to the immobilization of the molecular catalyst. This work is a step toward a systematic investigation of chemical functionality of carbon substrates, and chemical environment for heterogenized molecular catalysts. Herein, we study InPP immobilized on different carbon materials, basal-plane pyrolytic graphite (PG), glassy carbon (GC) and boron doped diamond (BDD), and evince the important role of the substrate, its pretreatment and the use of polymer membranes for immobilization, on the CO_2RR performance. The current work demonstrates the improvement of CO_2RR performance on heterogenized indium(III) protoporphyrin IX by modifying the substrate, its chemical functionality, and chemical environment of the catalyst. The findings can function as a first step in trying to improve other heterogenized molecular systems as well.

6.2 Experimental

The electrochemical experiments were carried out with a potentiostat (IviumStat or CompactStat, Ivium Technologies), in a conventional three-electrode cell, where the working electrode (WE) and counter electrode (CE) compartments were separated by a nafion membrane (Nafion 115). Basal-plane pyrolytic graphite, glassy carbon, and boron doped diamond discs (5, 5, 10 mm diameter respectively) were used as WE. The counter and reference electrode (RE) were a platinum wire and a reversible hydrogen electrode respectively. For correct measurements versus the RHE scale, the luggin capillary and the RHE compartment were filled with CO_2 saturated electrolyte before CO_2 reduction. The electrolyte is 0.1 M phosphate buffer of pH

9.6 ± 0.1, prepared with K_2HPO_4, K_3PO_4 and ultrapure water (Millipore MilliQ gradient A10 system, 18.2 MΩ·cm). The choice for this pH was based on the enhanced HCOOH selectivity observed previously.[12] The reported current densities were always normalized by the geometric surface area of the WE, and in some cases additional normalization by the amount of active species was performed for correct comparison of the activity. The potentials were corrected for ohmic drop by the potentiostat during measurement. Generally, potentiostatic bulk electrolysis was performed at E = -1.5 V vs. RHE for 90 minutes, with manual collection of 100 μl samples at certain times, and analyzed by High Performance Liquid Chromatography. The reported concentrations of liquid products, or subsequently calculated faradaic efficiency (FE) are an average of 3 - 5 independent experiments with freshly prepared electrodes. Additionally, the data points for each experiment were obtained by the average of three injections of the same sample. The dominant contribution of the uncertainty in concentration/FE resulted from the different experiments. Additional experimental details can be found in Appendix C.

6.3 Results and Discussion

6.3.1 Substrate effect

We compare the selectivity and activity for CO_2RR on InPP immobilized on PG, GC and BDD substrates. The immobilization procedure and amount of InPP dropcasted per cm^2 were kept the same for all the substrates (details in the SI). From the faradaic efficiency toward HCOOH, given in Figure 6.1a, it is observed that the substrate has a significant influence on the selectivity of CO_2RR on immobilized InPP. The PG substrate is the most selective toward HCOOH, and the GC substrate the least selective. These effects cannot be ascribed to the activity of the bare substrate as shown by control experiments in Figure C.17a, which show that bare PG, GC and BDD are not active for CO_2RR. In Figure 6.1b-d, the absolute total and partial current densities are shown for CO_2RR on the different substrates. For a correct comparison of the activity, the current density was also normalized by the real amount of InPP adsorbed on the substrate. As will be discussed in detail later, the electroactive coverage of InPP is not the same for the different substrates. It can be seen that there is an order of magnitude difference in j_{total} and j_{HCOOH} on PG compared to GC and BDD. Note that this difference is not associated to a difference in electrochemical active surface area (ECSA), as shown in Figure C.8(a). The fact that GC and BDD both perform worse compared to PG, indicates that the enhancement in CO_2RR selectivity and activity cannot be ascribed to either the high content of sp^2 or sp^3 carbon atoms present in respectively GC and BDD.

The results in Figure 6.1 are in line with the online mass spectrometry and online HPLC experiments, depicted in Figure 6.2a and b respectively, from which we confirm that significantly more H_2 is produced on InPP-GC, and significantly more HCOOH on InPP-PG. The CO_2 consumption on InPP-PG is also much

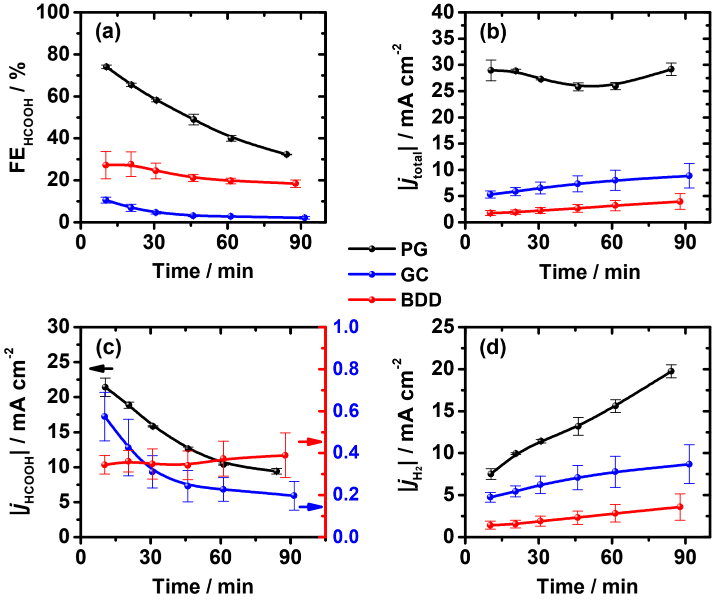

Figure 6.1 (a) Faradaic efficiency toward HCOOH, (b) absolute total current density, (c) absolute partial current density for HCOOH, and (d) absolute partial current density for H_2 during CO_2 reduction on immobilized InPP on different substrates in 0.1 M phosphate buffer of pH 9.6. Lines to guide the eye.

higher compared to the other substrates, in agreement with higher j_{total}, and the higher HCOOH production rate observed on PG compared to the other substrates. Although difficult to quantify, the onset potential for H_2 and HCOOH on InPP-BDD is at more negative potential compared to PG and GC, which is a general characteristic of BDD. Moreover, in Figure 6.2b we can observe differences in the peak potentials of HCOOH formation between the different substrates, which is related to the competition of the hydrogen evolution reaction (HER).

Besides a change in selectivity and activity, there is a clear difference in stability between the substrates, since a slight decrease is observed in j_{HCOOH} as a function of time on PG and GC, accompanied with an increase in j_{H_2}. We define the relative FE with respect to the initial value (Equation 6.1) as a measure for the stability of the system. From a graph of this relative FE versus time (Figure 6.3a), we can compare experiments with different values of FE. A more horizontal trend indicates a higher stability as the FE does not decrease significantly in time.

$$\frac{FE_t}{FE_{initial}} \times 100\% \tag{6.1}$$

The tendency of the FE to decrease with time has been observed before, and was associated with the detachment of InPP from the surface or deactivation of the

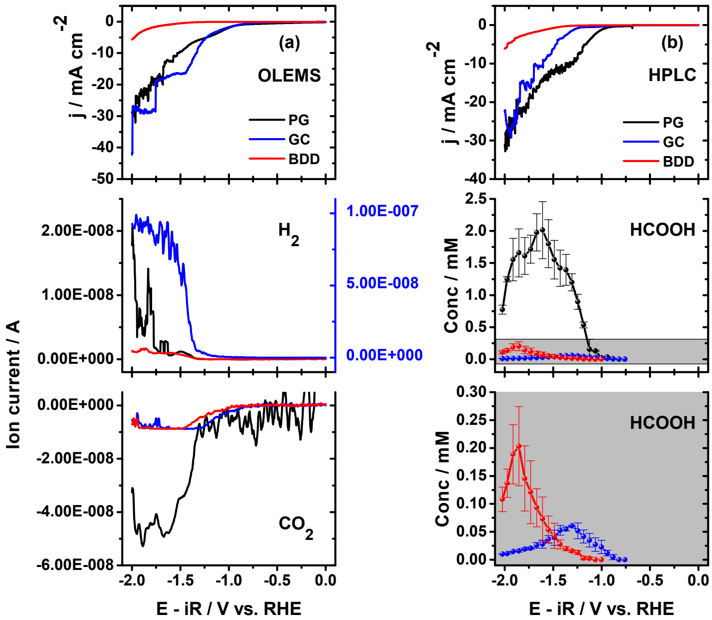

Figure 6.2 (a) Online Electrochemical Mass Spectrometry and (b) online HPLC during CO_2 reduction on immobilized InPP on different substrates in 0.1 M phosphate buffer of pH 9.6.

porphyrin.[12] We have performed x-ray photoelectron spectroscopy on InPP-PG before and after electrolysis, as shown in Figure 6.3b. We observed that the indium content on the electrode, which is a measure of the actual amount of InPP adsorbed on PG, is substantially decreased after 10 minutes, with a negligible further decrease after 1 hour, which is in agreement with the decreasing trend of FE as a function of time. Additionally, we performed experiments under homogeneous conditions of InPP (Figure C.4), in which we do not observe a decrease in selectivity with time. Therefore we confirm that the destabilization of immobilized indium protoporphyrin is related to detachment from the surface. Moreover, the detachment from the surface takes place in the first 10 minutes of electrolysis. The adsorption of the porphyrin on the substrate is through noncovalent π-π interactions,[30,38,39] which is believed to be important for enhanced CO_2RR performance, and strongly dependent on the carbon substrate.

We believe that the substrate morphology plays an important role as evidenced by the higher CO_2 consumption observed with OLEMS, which can be explained by efficient mass transport effects due to the more porous structure of PG compared to GC or BDD (Figure C.8a), which may also suppress the HER. These observations are similar to mass transport effects recently reported for heterogeneous electrocatalysts, showing that the mesostructure can affect the selectivity and activity of

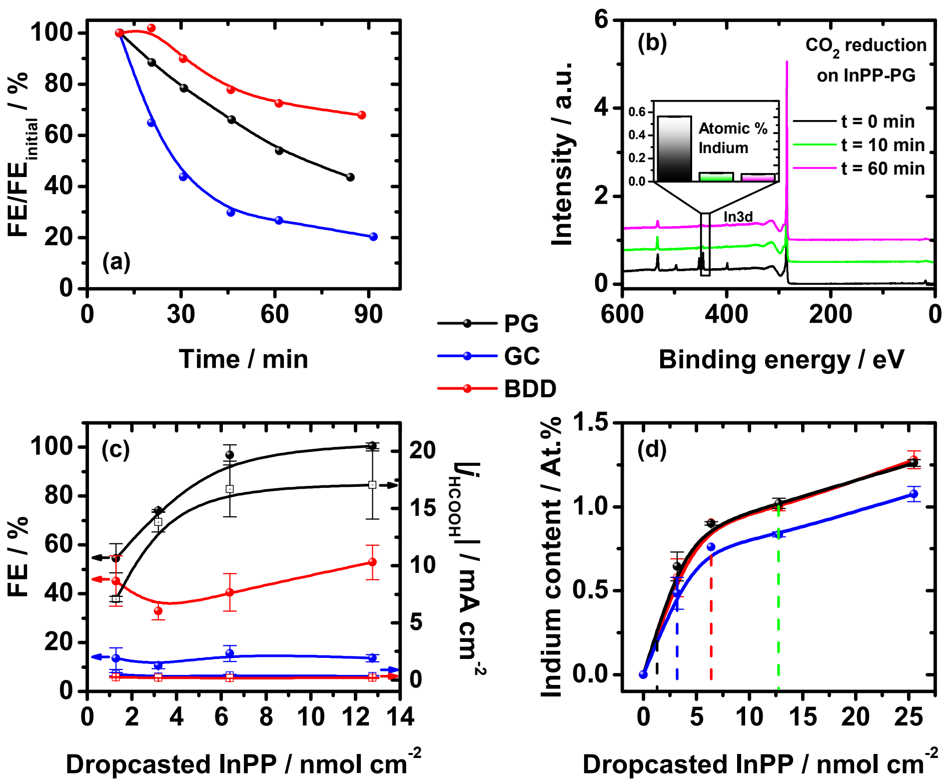

Figure 6.3 (a) Stability of immobilized InPP on different substrates (lines to guide the eye), (b) XPS spectra of InPP-PG electrodes before electrolysis and after electrolysis (t = 10 min and t = 1 h) with in the inset the indium content (at.%), (c) faradaic efficiency toward HCOOH (left axis) and partial current density for HCOOH (right axis) as a function of the amount InPP dropcasted on the different substrates (lines to guide the eye), and (d) indium content of the InPP immobilized on the substrates, as estimated from XPS, as a function of the amount InPP dropcasted (lines to guide the eye).

CO_2RR.[40,41] Additionally, a typical characteristic of GC is its poor permeability for gases, which likely affects the mass transport.[42] X-ray diffractometry and Raman spectroscopy of our substrates (Figure C.9a and C.10) indicate typical characteristics in agreement with the literature. PG and BDD exhibit sharp XRD peaks, and GC weak and broad peaks, indicating a high degree of crystallinity for PG and BDD, and a somewhat amorphous structure for GC.[43] The Raman spectra indicate the characteristic D- and G bands for sp^2 carbons in PG, and a specific peak associated to sp^3 carbon in BDD. The Raman bands for GC are weaker and less sharp, which indicate disorder of the graphite lattice for GC.[44,45] The low activity and selectivity on GC may be associated with its poor crystallinity, as a high crystallinity infers enhanced charge transport, as observed in covalent organic frameworks.[29,46] Recently, crystallinity has been shown to play an important role on the selectivity of CO_2RR on copper phthalocyanine catalysts.[47] However, high crystallinity alone is not sufficient for improved CO_2RR catalysis, based on the significant differences in CO_2RR performance between PG and BDD, which are both highly crystalline.

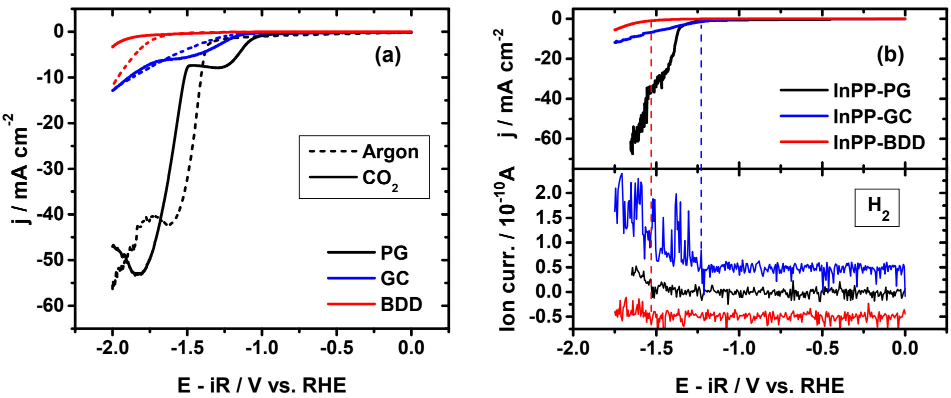

Figure 6.4 (a) Linear sweep voltammetry on immobilized InPP on different substrates in 0.1 M phosphate buffer of pH 9.6 under argon and CO_2 atmosphere, scan rate: 20 mV s^{-1} and (b) Online Electrochemical Mass Spectrometry measurement of hydrogen evolution on InPP immobilized on different substrates

Apart from the substrate morphology and surface structure, a plausible explanation for the enhanced selectivity and activity on PG may be related to a difference in the effective amount of the porphyrin on the three substrates. As can be seen in Figure 6.3c, a difference in the amount of immobilized InPP on the substrate leads to a difference in activity and selectivity (details of the corresponding experiments are provided in Figures C.1-C.3). In case of PG this concentration effect is more pronounced, and in case of GC almost completely absent, which can be interpreted as a ”InPP saturation limit” that is reached earlier for GC compared with PG. In other words, PG substrate can accommodate more catalyst compared to GC and BDD. These conclusions are in agreement with quantitative information obtained from XPS spectra of InPP immobilized on the different substrates (Figure C.12). We also varied the amount of InPP dropcasted on the different substrates and plotted the indium content as estimated by XPS vs. the amount dropcasted in Figure 6.3d. The vertical dashed lines indicate the InPP amounts used for the qualitative study shown in Figure 6.3c and C.1-C.3. It can be seen that the indium content is the highest for PG and the lowest for GC, which is in agreement with our conclusion that a PG substrate can accommodate more catalyst compared to GC. Furthermore, we used the indium content of InPP immobilized on different substrates (PG, GC, BDD = 0.65, 0.49, 0.58) to normalize the activity to real amount of adsorbed InPP (Figure 6.1b-d).

Another cause of the improved CO_2RR selectivity may be a difference in HER activity between the substrates instead of solely an intrinsic substrate effect specifically related to CO_2RR. In Figure 6.4a, a comparison between the substrates for HER and CO_2RR is shown. The high overpotential for HER on the BDD substrate does not favor CO_2RR, since the CO_2RR onset potential is shifted toward more negative potentials, and the current is suppressed on InPP-BDD with CO_2 in solution. The HPLC results (Figure 6.2b) confirm the formation of HCOOH at more negative potentials on BDD compared to GC and PG. Under argon, where only hydrogen evolution takes place, the current density on InPP-GC is smaller compared to InPP-PG. However, as shown by OLEMS measurements in Figure 6.4b, more H_2 is produced on GC. Moreover, in the presence of CO_2, the onset potential is shifted positively for InPP-PG, but is almost unchanged for InPP-GC, which indicates a more efficient catalysis of CO_2RR on PG with respect to GC, in agreement with the online experiments in Figure 6.2. Consequently, the GC substrate is more active toward HER compared to PG. These results indicate that the competition between CO_2RR and HER strongly depends on the nature of the substrate, which in turn affects HCOOH selectivity.

In order to increase the impact and generality of our findings, we studied the substrate effect on protoporphyrins with Rh and Sn metal centers, which previously were found to produce HCOOH.[12] Although the HCOOH selectivity for these porphyrins is much lower than for InPP (which is an intrinsic catalytic effect), a similar trend can be observed for the different substrates as found for InPP (Figure C.5). Pyrolytic graphite substrate leads to the highest FE, while glassy carbon substrate is the least selective toward HCOOH.

The above results demonstrate the important influence of the substrate, which is believed to be the result of an interplay of several factors influencing the selectivity and reactivity of CO_2RR, such as morphology/mesostructure (and thereby optimized mass transport effects), crystallinity, electrostatic interaction with the molecular catalyst, and activity for HER.

6.3.2 Effect of substrate pretreatment

Besides the nature of the substrate, modification or treatment of the substrate surface offers a means to influence the CO_2 selectivity, reactivity, and stability. We investigated the influence of a cathodic and anodic electrochemical pretreatment ("Cat-PG" and "An-PG"), and a H_2 and O_2 plasma treatment ("H_2-PG" and "O_2-PG") of the PG substrate. In Figure 6.5, it is shown that O_2 plasma treatment increases the FE and j_{HCOOH}. These effects can be attributed to a change in chemical functionality as discussed later, instead of an increased surface area as evidenced by similar C_{dl} before and after O_2 plasma treatment (Figure C.8b). Furthermore, the exposure time of O_2 plasma seems to play a role as shown in Figure C.6, since a mild O_2 plasma treatment (3 and 6 min. exposure) slightly

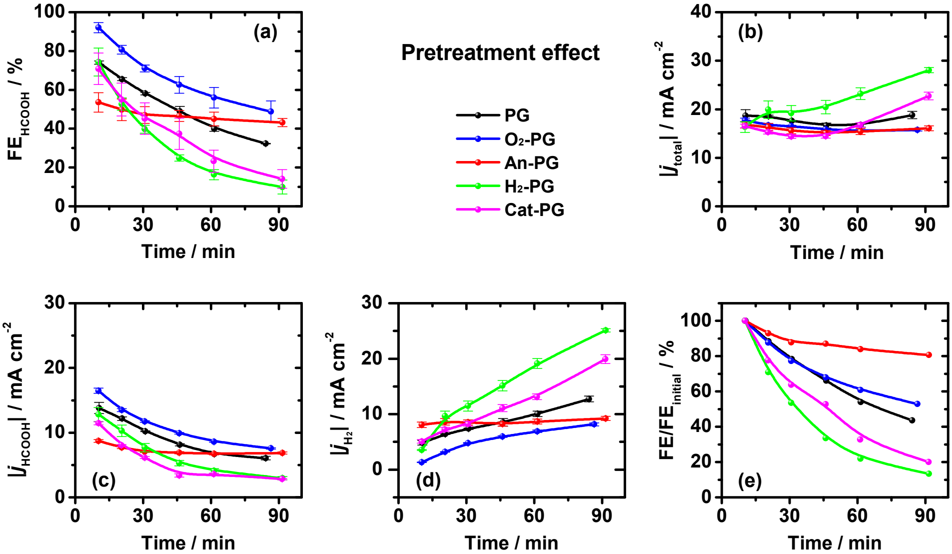

Figure 6.5 (a) Faradaic efficiency toward HCOOH, (b) absolute total current density, (c) absolute partial current density for HCOOH, (d) absolute partial current density for H_2, (e) stability during CO_2 reduction on immobilized InPP on different pretreated PG substrates. Electrolyte: 0.1 M phosphate buffer of pH 9.6. Lines to guide the eye.

improves CO_2RR, while a harsh O_2 plasma treatment (12 min exposure) worsens CO_2RR performance. In Figure 6.5e, it is shown that O_2 plasma treatment has negligible influence on the stability. Anodization of PG leads to lower initial FE, but improves the stability dramatically. Moreover, both hydrogen treatments, cathodic and H_2 plasma, decrease the selectivity, reactivity and stability of CO_2RR significantly. Since H_2-PG has a lower C_{dl} and thus a smaller surface area (Figure C.8b), but a higher j_{total}, the observed changes in selectivity and reactivity do not result from a change in surface area of PG after H_2 plasma treatment.

The observed differences for the investigated pretreated PG substrates, highlight the role of oxygenated and hydrogenated functional groups of the substrate's surface on the immobilization of InPP and subsequently on the CO_2RR. Our results imply that hydrogen functional groups on the PG surface strongly decrease CO_2RR selectivity, reactivity and stability, and oxygen functionalities increase CO_2RR performance. H_2 plasma consists of a large amount of H atoms, which reacts with surface oxides leading to C-H bonds and a decreased O/C ratio on the surface.[24,48] The chemisorbed hydrogen on the surface promotes HER with respect to CO_2RR, which is reflected in a decrease in FE and j_{HCOOH}, and increase in j_{H_2}. On the other hand, O_2 plasma treatment increases the amount of oxygen functional groups (e.g. hydroxyl, carbonyl, carboxylate) on the surface, which generally leads to a more polar and hydrophilic surface and stronger adsorbate-substrate interaction.

O_2 plasma treated PG shows an improvement in CO_2RR selectivity. A similar influence of O_2 plasma treatment of the substrate has been reported before for the oxygen reduction reaction.[49]

On anodically treated PG we expected similar behavior as after O_2 plasma treatment, due to the introduction of oxygenated species, but no improvement in activity or selectivity has been observed. However, a remarkable increase in the stability is observed. Based on blank voltammograms of the pretreated PG (Figure C.7), there is a significant difference in An-PG compared to the untreated and other pretreated PG electrodes. Application of strong anodic pretreatment causes a destruction of the carbon surface, and formation of a thick graphite oxide layer, which contains a high amount of anionic sites and interior void volume, leading to high surface area, in agreement with the dramatic increase in C_{dl} for An-PG in Figure C.8b.[24,50] Complementary information was obtained by x-ray diffractometry, Raman spectroscopy, and x-ray photoelectron spectroscopy. As shown in Figure C.9b, the crystalline nature of PG remains intact upon electrochemical pretreatment. However, anodization of PG leads to a significant increase in the Raman peak at $\approx$ 1352 cm^{-1}, and a slight increase in the D' peak around 1620 cm^{-1} (Figure C.10b). The peak at 1352 cm^{-1} is attributed to the presence of graphitic edges, which increases in intensity upon anodic treatment as observed in our spectra, and the peak at 1620 cm^{-1} indicates delamination of graphitic planes. Formation of graphite oxide increases the strain on the PG lattice, leading to fracturization.[51] In Figure C.11 the ratio of the D- and G band intensity for the different substrates and pretreated PG is depicted, which clearly shows a high ratio of I_D/I_G in case of An-PG. Anodization of PG leads to an increase in the edge plane density. Note that GC also exhibits a relatively high I_D/I_G, but showed a poor stability as seen before. Therefore, we believe a high edge plane density in combination with high crystallinity to be the reason for the strongly improved stability. The XPS spectra of the plasma- and electrochemically treated pyrolytic graphite electrodes, shown in Figure C.13, provide a quantitative basis for our conclusions about chemical functionality on CO_2RR performance. The oxygen content is significantly higher on An-PG and O_2-PG compared to untreated PG. Moreover, the H_2 plasma- and cathodically treated PG exhibit less surface oxygenated species compared to untreated PG. These results are in agreement with our interpretation of the CO_2RR results and our Raman spectroscopy experiments.

6.3.3 Effect of polymer encapsulation

In addition to pretreating the substrate, another strategy aimed at improving CO_2RR selectivity, reactivity and stability, is by incorporation of the porphyrin in polymeric matrices. In this work, we compare the influence of didodecyldimethylammonium bromide (DDAB), nafion®, poly(4-vinylpyridine) (P4VP), and poly(3,4-ethylenedioxythiophene) polystyrene sulfonate (PEDOT:PSS). Details about the immobilization in these polymeric matrices are given in the SI. The concentration of InPP in the polymer films, and the amount of polymer dropcasted per cm^2 surface

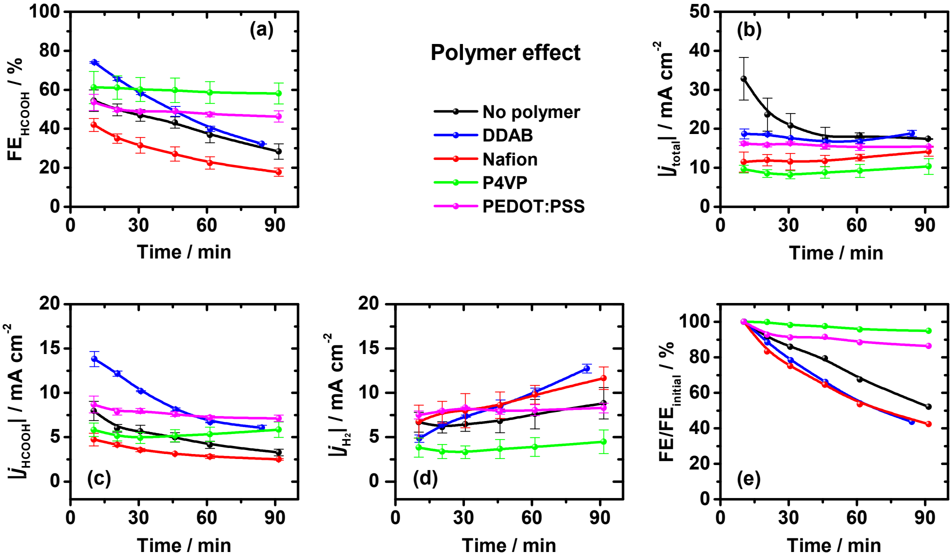

Figure 6.6 (a) Faradaic efficiency toward HCOOH, (b) absolute total current density, (c) absolute partial current density for HCOOH (d) absolute partial current density for H_2, (e) stability during CO_2 reduction on immobilized InPP in different polymer membranes. Electrolyte: 0.1 M phosphate buffer of pH 9.6. Lines to guide the eye.

were always kept the same. As depicted in Figure 6.6, interesting differences are observed between the polymer membranes. Compared with polymer-free InPP (InPP-PG), encapsulation in DDAB, P4VP, and PEDOT:PSS shows enhanced selectivity and activity, whereas nafion negatively impacts the selectivity and activity. From Figure 6.6d it can be seen that the HER activity with P4VP is drastically decreased. A striking observation in Figure 6.6e is the enhanced stability when using P4VP or PEDOT:PSS compared to the other polymers. These results underscore the importance of the nature of the polymer as seen before for a modified bulk silver electrode.[52] Enhanced CO_2RR performance by P4VP has been reported before for cobalt phthalocyanine, where the authors explain the observed effects by the presence of pyridine residues in the polymer, which influences the coordination to the catalyst.[35,36] Although nafion coated catalysts are widely used for various electrocatalytic systems, negative effects of nafion on the catalytic activity have been observed previously.[53,54]

Differences in polymer-dispersed catalysts are generally associated with the introduction of a hydrophobic environment, leading to the suppression of the HER.[28,34,55] However, the differences in CO_2RR performance in our investigation are likely to be explained by the different chemical structures of the polymers (Figure C.14), leading to different substrate/adsorbate interactions. As can be seen in the blank CVs in Figure C.15, the typical InPP peaks are masked or shifted for nafion, P4VP and PEDOT:PSS. Changes in the voltammetric behavior after immobilization of porphyrins in DDAB have been reported before, in which the authors also suggest the possibility of porphyrin dimer formation in DDAB vesicles.[55] The absence of InPP redox peaks in the investigated potential window indicates a change in electrochemical behavior, but does not rule out the presence of InPP on the surface since reasonable amounts of HCOOH are produced. The CV of PEDOT:PSS coated PG shows a much larger double layer, which indicates the strong influence of the polymer on the chemical environment near the electrode surface. The polymers without InPP exhibit reasonable CO_2RR activity as can be seen in Figure C.17b, where the same trend is observed as for InPP encapsulated in the different polymers. A detailed investigation of the electrocatalytic activity of polymers for CO_2RR is beyond the aim of this work. Nonetheless, it can be concluded that the observed effects are partly due to the activity of the polymer for CO_2RR, which is higher with P4VP and PEDOT:PSS. The pyridine group in P4VP and aromatic moieties in PEDOT:PSS are assumed to play an important role in this respect, since Dunwell et al. very recently reported CO_2RR toward HCOOH mediated by pyridine.[56] The porphyrin exhibits a planar macrocycle with large π-conjugation, which facilitates electrostatic interactions with the polymer. We believe that the increased stability is a result of the presence of aromatic building blocks as present in P4VP and PEDOT:PSS, which facilitates axial coordination to the indium metal center by electron donation. This effect is known for pyridine or imidazole ligands which are used for (covalently) anchoring catalysts to electrodes, and are found to stabilize the coordination of CO_2.[34] This interaction is absent in case of Nafion and DDAB, leading to a inferior stability compared to the polymer-free InPP, P4VP and PEDOT:PSS. DDAB shows an increase in selectivity and activity, which is associated with the suppression of the HER similar to previous work.[52] The poor CO_2RR performance with nafion is tentatively ascribed to the low mobility of the porphyrin in the polymer, and a disordered structure of the nafion layer.[53,54] We performed electrochemical impedance spectroscopy on the different polymer dispersed catalysts to investigate the kinetics of electron-transfer processes (Figure C.16). As discussed in the SI, the charge transfer resistance between the polymer films is in agreement with the observed activity in Figure 6.6b. We conclude that the nature of the polymer affects the rate of electron transfer during CO_2RR rather than mass transport of active species, leading to different activity amongst the polymer films.

The results in the present work demonstrate that the hydrophobic environment, induced by the polymer membrane in general, not always leads to suppression of the HER activity and subsequent improvement of CO_2RR. Additional effects related to the chemical structure, allowing for electrostatic interactions with the porphyrin or activity towards CO_2RR by the polymer itself, play an important role. Note that the current findings strongly depend on the (molecular) catalyst under study, and one should be careful to generalize the observed polymer effects for other electrocatalytic systems. Nonetheless, we emphasize the possible negative influence of nafion on CO_2RR, as nafion is very often used to immobilize catalysts, or as binder in the preparation of ink containing nanoparticulate electrocatalysts.

6.4 Conclusions

This work has shown the importance of the nature of the substrate for immobilized indium(III) protoporphyrin IX for CO_2RR toward formic acid. For this particular system, a pyrolytic graphite substrate outperforms glassy carbon and boron doped diamond in terms of CO_2RR selectivity and reactivity, while boron doped diamond shows the best stability. The enhanced activity and selectivity of PG are assigned to a combination of different factors. First, to a more porous surface structure, leading to efficient mass transport. Furthermore, to an optimal interaction between substrate and InPP, and a favorably low HER activity.

We have investigated two strategies to improve or alter the selectivity, reactivity, and stability of CO_2RR. Pretreatment of the substrate before catalyst immobilization, and immobilization in polymeric matrices have shown to be practical tools to fine-tune CO_2 reduction performance. Hydrogenated functional groups on the surface decrease the selectivity, activity, and stability, while (mild) oxygen functionalization positively influences the CO_2 reduction performance. Anodization of the graphite surface substantially increases the stability, which is believed to be related to the thick graphite oxide layer containing high edge plane density. Both P4VP and PEDOT:PSS, increase the stability, which is believed to be due to axial coordination of their aromatic moieties to the indium metal center. DDAB, P4VP and PEDOT:PSS improve the performance of CO_2RR, while nafion impacts CO_2RR negatively. These strategies are assumed to be applicable to similar macrocyclic catalysts immobilized on carbon materials.

It should be noted that the CO_2RR performance is often a trade-off between selectivity, activity, and stability, each of which can be modified by substrate pretreatment and catalyst encapsulation in polymers. Although complete mechanistic insight in the pretreatment- and polymer effects is still missing, the results obtained here, may help to design heterogenized molecular catalytic systems for CO_2 reduction with specifically optimized properties. Other molecular catalysts may behave differently, hence one should be careful generalizing the results obtained in this study. However, it is very likely that the substrate, its pretreatment, and catalyst dispersion in polymers will have an influence on CO_2RR performance, and the insight obtained herein may be used as starting point for further optimization of the system.

6.5 References

[1] D. T. Whipple, P. J. A. Kenis, *J. Phys. Chem. Lett.* **2010**, *1*, 3451–3458.

[2] J.-P. Jones, G. K. S. Prakash, G. A. Olah, *Isr. J. Chem.* **2014**, *54*, 1451–1466.

[3] J. Durst, A. Rudnev, A. Dutta, Y. Fu, J. Herranz, V. Kaliginedi, A. Kuzume, A. A. Permyakova, Y. Paratcha, P. Broekmann, T. J. Schmidt, *Chimia* **2015**, *69*, 769–776.

[4] R. Kortlever, J. Shen, K. J. P. Schouten, F. Calle-Vallejo, M. T. M. Koper, *J. Phys. Chem. Lett.* **2015**, *6*, 4073–4082.

[5] J. P. Collin, J P Sauvage, *Coord. Chem. Rev.* **1989**, *93*, 245–268.

[6] E. E. Benson, C. P. Kubiak, A. J. Sathrum, J. M. Smieja, *Chem. Soc. Rev.* **2009**, *38*, 89–99.

[7] C. Finn, S. Schnittger, L. J. Yellowlees, J. B. Love, *Chem. Commun.* **2012**, *48*, 1392–1399.

[8] J. Bonin, A. Maurin, M. Robert, *Coord. Chem. Rev.* **2017**, *334*, 184–198.

[9] J.-M. Savéant, *Chem. Rev.* **2008**, *108*, 2348–2378.

[10] N. Furuya, K. Matsui, *J. Electroanal. Chem.* **1989**, *271*, 181–191.

[11] L. Chen, Z. Guo, X.-G. Wei, C. Gallenkamp, J. Bonin, E. Anxolabéhère-Mallart, K.-C. Lau, T.-C. Lau, M. Robert, *J. Am. Chem. Soc.* **2015**, *137*, 10918–10921.

[12] Y. Y. Birdja, J. Shen, M. T. M. Koper, *Catal. Today* **2017**, *288*, 37–47.

[13] S. Yamazaki, Y. Yamada, S. Takeda, M. Goto, T. Ioroi, Z. Siromaa, K. Yasuda, *Phys. Chem. Chem. Phys.* **2010**, *12*, 8968–8976.

[14] C. Costentin, S. Drouet, M. Robert, J.-M. Savéant, *Science* **2012**, *338*, 90–94.

[15] A. Lü, Y. Fang, M. Zhu, S. Huang, Z. Ou, K. M. Kadish, *J. Porphyrins Phthalocyanines* **2012**, *16*, 310–315.

[16] I. Azcarate, C. Costentin, M. Robert, J.-M. Savéant, *J. Am. Chem. Soc.* **2016**, *138*, 16639–16644.

[17] Z. N. Zahran, E. A. Mohamed, Y. Naruta, *Scientific Reports* **2016**, *6*, 1–12.

[18] J. L. Inglis, M. T. MacLean, B. J. Pryce, J. G. Vos, *Coord. Chem. Rev.* **2012**, *256*, 2571–2600.

[19] G. F. Manbeck, E. Fujita, *J. Porphyrins Phthalocyanines* **2015**, *19*, 45–64.

[20] J. Shen, R. Kortlever, R. Kas, Y. Y. Birdja, O. Diaz-Morales, Y. Kwon, I. Ledezma-Yanez, K. J. P. Schouten, G. Mul, M. T. M. Koper, *Nat. Commun.* **2015**, *6*, 8177.

[21] S. A. Yao, R. E. Ruther, L. Zhang, R. A. Franking, R. J. Hamers, J. F. Berry, *J. Am. Chem. Soc.* **2012**, *134*, 15632–15635.

[22] A. Morozan, S. Campidelli, A. Filoramo, B. Jousselme, S. Palacin, *Carbon* **2011**, *49*, 4839–4847.

[23] S. Navalón, J. R. Herance, M. Álvaro, H. García, *Chem. Eur. J.* **2017**, *23*, 1–33.

[24] R. L. McCreery, *Chem. Rev.* **2008**, *108*, 2646–2687.

[25] M. L. Rigsby, D. J. Wasylenko, M. L. Pegis, J. M. Mayer, *J. Am. Chem. Soc.* **2015**, *137*, 4296–4299.

[26] T. V. Magdesieva, T. Yamamoto, D. A. Tryk, A. Fujishima, *J. Electrochem. Soc.* **2002**, *149*, D89–D95.

[27] R. W. Murray, *Acc. Chem. Res.* **1980**, *13*, 135–141.

[28] R. W. Murray, A. G. Ewing, R. A. Durst, *Anal. Chem.* **1987**, *59*, 379A–390A.

[29] S. Lin, C. S. Diercks, Y.-B. Zhang, N. Kornienko, E. M. Nichols, Y. Zhao, A. R. Paris, D. Kim, P. Yang, O. M. Yaghi, C. J. Chang, *Science* **2015**, *349*, 1208–1213.

[30] Z. Sun, L. Kong, X. Ding, C. Du, X. Zhao, J. Chen, H. Fu, X. Yang, T. Cheng, *Phys. Chem. Chem. Phys.* **2016**, *18*, 9367–9376.

[31] C. W. Li, M. W. Kanan, *J. Am. Chem. Soc.* **2012**, *134*, 7231–7234.

[32] Y. Chen, C. W. Li, M. W. Kanan, *J. Am. Chem. Soc.* **2012**, *134*, 19969–19972.

[33] H. Mistry, A. S. Varela, C. S. Bonifacio, I. Zegkinoglou, I. Sinev, Y.-W. Choi, K. Kisslinger, E. A. Stach, J. C. Yang, P. Strasser, B. R. Cuenya, *Nat. Commun.* **2016**, *7*, 12123.

[34] T. Abe, T. Yoshida, S. Tokita, F. Taguchi, H. Imaya, M. Kaneko, *J. Electroanal. Chem.* **1996**, *412*, 125–132.

[35] T. Yoshida, K. Kamato, M. Tsukamoto, T. Iida, D. Schlettwein, D. W. M. Kaneko, *J. Electroanal. Chem.* **1995**, *385*, 209–225.

[36] W. W. Kramer, C. C. L. McCrory, *Chem. Sci.* **2016**, *7*, 2506–2515.

[37] J.-M. Savéant, *ChemElectroChem* **2016**, *3*, 1967–1977.

[38] J.-H. Fuhrhop, *Langmuir* **2014**, *30*, 1–12.

[39] A. Maurin, M. Robert, *J. Am. Chem. Soc.* **2016**, *138*, 2492–2495.

[40] R. Kas, K. K. Hummadi, R. Kortlever, P. de Wit, A. Milbrat, M. W. Luiten-Olieman, N. E. Benes, M. T. Koper, G. Mul, *Nat. Commun.* **2016**, *7*, 10748.

[41] Y. Yoon, A. S. Hall, Y. Surendranath, *Angew.Chem. Int.Ed.* **2016**, *55*, 15282–15286.

[42] F. C. Cowlard, D. C. Lewis, *J. Mater. Sci.* **1967**, *2*, 507–512.

[43] Y. Hishiyama, M. Nakamura, *Carbon* **1995**, *33*, 1399–1403.

[44] R. Bowling, R. T. Packard, R. L. McCreery, *Langmuir* **1989**, *5*, 683–688.

[45] Y. Wang, D. C. Alsmeyer, R. L. McCreery, *Chem. Mater.* **1990**, *2*, 557–563.

[46] S. Wan, F. Gándara, A. Asano, H. Furukawa, A. Saeki, S. K. Dey, L. Liao, M. W. Ambrogio, Y. Y. Botros, X. Duan, S. Seki, J. F. Stoddart, O. M. Yaghi, *Chem. Mater.* **2011**, *23*, 4094–4097.

[47] S. Kusama, T. Saito, H. Hashiba, A. Sakai, S. Yotsuhashi, *ACS Catal.* **2017**, *7*, 8382–8385.

[48] J. Xu, Q. Chen, G. M. Swain, *Anal. Chem.* **1998**, *70*, 3146–3154.

[49] K. Vaik, D. J. Schiffrin, K. Tammeveski, *Electrochem. Commun.* **2004**, *6*, 1–5.

[50] R. S. Kelly, D. J. Weiss, S. H. Chong, T. Kuwana, *Anal. Chem.* **1999**, *71*, 413–418.

[51] R. Bowling, R. T. Packard, R. L. McCreery, *J. Am. Chem. Soc.* **1989**, *111*, 1217–1223.

[52] F. Quan, M. Xiong, F. Jia, L. Zhang, *Appl. Surf. Sci.* **2017**, *399*, 48–54.

[53] D. A. Buttry, F. C. Anson, *J. Am. Chem. Soc.* **1984**, *106*, 59–64.

[54] A. Jarzębińska, P. Rowiński, I. Zawisza, R. Bilewicz, L. Siegfried, T. Kaden, *Analytica Chimica Acta* **1999**, *396*, 1–12.

[55] M. T. de Groot, M. T. M. Koper, *Phys. Chem. Chem. Phys.* **2008**, *10*, 1023–1031.

[56] M. Dunwell, Q. Lu, J. M. Heyes, J. Rosen, J. G. Chen, Y. Yan, F. Jiao, B. Xu, *J. Am. Chem. Soc.* **2017**, *139*, 3774–3783.